Long wavelength gradient drift instability in Hall plasma devices. I. Fluid theory

Winston Frias, Andrei I. Smolyakov, Igor D. Kaganovich, and Yevgeny Raitses

Citation: Physics of Plasmas (1994-present) **19**, 072112 (2012); doi: 10.1063/1.4736997
View online: http://dx.doi.org/10.1063/1.4736997
View Table of Contents: http://scitation.aip.org/content/aip/journal/pop/19/7?ver=pdfcov
Published by the AIP Publishing

Long wavelength gradient drift instability in Hall plasma devices. I. Fluid theory

Winston Frias,[1,a)] Andrei I. Smolyakov,[1] Igor D. Kaganovich,[2] and Yevgeny Raitses[2]
[1]*Department of Physics and Engineering Physics, University of Saskatchewan, 116 Science Place Saskatoon, SK S7N 5E2, Canada*
[2]*Princeton Plasma Physics Laboratory, Princeton, New Jersey 08543, USA*

(Received 22 February 2012; accepted 11 June 2012; published online 18 July 2012)

The problem of long wavelength instabilities in Hall thruster plasmas is revisited. A fluid model of the instabilities driven by the $\mathbf{E}_0 \times \mathbf{B}$ drift in plasmas with gradients of density, electron temperature, and magnetic field is proposed. It is shown that full account of compressibility of the electron flow in inhomogeneous magnetic field leads to quantitative modifications of earlier obtained instability criteria and characteristics of unstable modes. Modification of the stability criteria due to finite temperature fluctuations is investigated. © *2012 American Institute of Physics*. [http://dx.doi.org/10.1063/1.4736997]

I. INTRODUCTION

Plasmas involving strong electron drift in crossed electric and magnetic fields are of great interest for a number of applications such as space propulsion and material processing plasma sources. In these devices, the strength of the external magnetic field is chosen such that electrons are magnetized, $\rho_e \ll L$, but ions are not, $\rho_i \gg L$, where L is the characteristic length scale of the plasma region in the device. Electron and ion dynamics are mostly collisionless, though inter-particle collisions (including those with neutrals) as well as with the walls can also be important. Similar conditions are also met in a variety of other plasmas such as in ionosphere, reconnecting magnetotail, shock waves, and pinch devices. For the purpose of this paper all these are loosely defined as Hall plasmas.

Hall plasma conditions are typical for many technological applications. Common feature of these devices is the presence of stationary, externally applied electric field $\mathbf{E}_0$, which is perpendicular to the equilibrium magnetic field $\mathbf{B}_0$, thus producing stationary $\mathbf{E}_0 \times \mathbf{B}_0$ drift velocity. The ions, due to large Larmor radius, are unmagnetized and accelerated in the $\mathbf{E}_0$ direction, while the electron collisions lead to a finite current along the $\mathbf{E}_0$. As a result, quasineutral plasma is accelerated along the $\mathbf{E}_0$. Such plasma accelerators, typically in coaxial geometry with radial magnetic field $\mathbf{B}_0$, axial $\mathbf{E}_0$, and azimuthal $\mathbf{E}_0 \times \mathbf{B}_0$ drift, also used as technological plasma sources, have recently became a subject of growing interest due to their applications in electric space propulsion, so called Hall plasma thrusters.

Hall plasma in externally applied electric field $\mathbf{E}_0$, which is perpendicular to the equilibrium magnetic field $\mathbf{B}_0$, is a basis for operation of Hall thrusters,[1–3] which are high efficiency, low thrust engines used on many missions for satellite orbit corrections, and planned for future interplanetary missions. Magnetron plasma discharges, which are widely used in materials processing for sputter deposition of metallic and insulating films, are also based on the electron drift in the crossed electric and magnetic fields in the presence of non-magnetized ions.

Despite many successful applications of Hall thrusters and other Hall plasma sources, some aspects of their operation are still poorly understood. A particularly important problem is the anomalous electron mobility,[4–6] which greatly exceeds classical collisional values. Hall plasma devices exhibit numerous turbulent fluctuations in a wide frequency range[7–10] and it is generally believed that fluctuations resulting from plasma instabilities are probable reasons of anomalous mobility.

An inhomogeneous plasma immersed in external inhomogeneous electric and magnetic fields is not in a state of thermodynamic equilibrium. The equilibrium $\mathbf{E}_0 \times \mathbf{B}_0$ electron drift is a source of a number of plasma instabilities in Hall plasmas.[11] There exists a large body of work devoted to studies of such instabilities in applications to shock waves in laboratory and space plasmas. These instabilities were observed in a number of experiments,[12,13] and thought to be responsible for anomalous resistance and turbulent heating. Low-hybrid instability and modified two-stream instability of Hall plasma with transverse current[14–16] are thought to be particularly important. Effects of plasma and magnetic field gradients on low hybrid instability were studied in kinetic theory in Refs. 17–20. The modified two-stream instability was studied in detail (also in kinetic theory) in Refs. 12 and 21. Lower hybrid instability is typically a short wavelength mode with $k_\perp \rho_e \simeq 1$, where ρ_e is the electron Larmor radius, while the modified two stream version has the most unstable modes for longer wavelengths $k_\perp \rho_e < 1$,[12] but requires a finite component of the wavevector along the magnetic field. The short wavelength low hybrid modes are also a special case of more general beam cyclotron instabilities,[21–23] in which higher cyclotron harmonics are included. Nonlinear stage of such cyclotron instabilities driven by the transverse current was analyzed in Refs. 21, 22, and 24, where it was concluded that these small scale modes saturate at relatively low amplitude due the ion trapping.

The $\mathbf{E}_0 \times \mathbf{B}_0$ instability driven by the combination of magnetic field and density gradients was experimentally and

a)Electronic mail: wpf274@mail.usask.ca.

theoretically identified as a possible source of fluctuations and anomalous mobility in Hall plasma thrusters.[25,26] This is the long wavelength instability obtained in neglect of the effects of electron inertia, $m_e \to 0$. Therefore, it is not directly related to the low hybrid modes, nor it requires a finite value of the wavevector along the equilibrium magnetic field, $k_{||}$. Later, theoretical studies revealed the existence of other instability mechanisms in Hall thrusters due to collisions and ionization,[27,28] Rayleigh type shear flow instability, and resistive instabilities of low-hybrid and Alfvén waves.[29,30] Kinetic studies[23] identified the high-frequency instability driven by the resonances between the electron cyclotron harmonics and $\mathbf{E}_0 \times \mathbf{B}_0$ drift.

In this paper, we revisit the problem of the long wavelength $\mathbf{E}_0 \times \mathbf{B}_0$ instability in plasmas with inhomogeneous magnetic field and gradients of plasma density gradients which was originally studied in Ref. 26 and more recently in Ref. 31. It is expected that, if present, long wavelength modes will dominate the anomalous transport of electrons. These modes have been originally proposed[25,26] as a possible cause of turbulent fluctuations and anomalous transport in Hall thruster. Recent experimental observations have confirmed presence of high frequency long wavelength modes,[5,32] however it is not clear whether the standard criteria for gradient density magnetic field driven instability instability[25,26,31] are satisfied everywhere inside the thruster channel.[33] We revisit the problem of gradient instability and show that quantitative corrections (to previous theory) are required for accurate determination of the conditions for the instability and its characteristics (real part of the frequency and the growth rate). Furthermore, we show that in inhomogeneous magnetic field the studied modes have finite perturbations of the electron temperature. We develop a three-field fluid model describing the fluctuations of the electric field, density, and electron temperature and study how finite temperature perturbations any affect the quantitative picture of instabilities. We investigate general stability criteria and in accompanying paper, Part II, study the stability of realistic profiles in some Hall thrusters.

In this paper, we concentrate on long wavelength modes existing in neglect of electron inertia and assuming $k_{||} = 0$, when low hybrid and modified two-stream instabilities are not operative. These assumptions are similar to those in previous works.[26,31] The instability of short wavelength modes in application to Hall thruster conditions (but without gradient effects) was considered in kinetic theory and numerical simulations in Refs. 23 and 34. It was shown that short wavelength modes are excited with some features similar to those observed by collective light scattering.[10,35] The analysis of Refs. 23 and 34 also included in part the effects of $k_{||} \neq 0$, which may be required in geometry of Hall thruster experiments. The extension of our analysis (of effects of plasma parameters and magnetic field gradients) into the short wavelength regime requires a kinetic theory and will be a subject of a separate publication.

The paper is organized as follows. In Sec. II, the instability due to density gradient is studied and a comparison with previous models is given. Section III discusses the effects of the electron temperature gradients and its role in the gradient-drift instabilities. The summary is given in Sec. IV.

II. LONG WAVELENGTH HALL PLASMA INSTABILITY DUE TO GRADIENTS OF DENSITY AND MAGNETIC FIELD

The gradients of plasma density and magnetic field were earlier identified as a source of robust instability in Hall thruster plasma with electron drift due to the equilibrium electric field. We consider this instability in this section and show that a more accurate analysis leads to a quantitatively different result as compared to previous works, though the physical mechanisms behind the instability remain similar.

We consider the simplified geometry of a coaxial Hall thruster with the equilibrium electric field $\mathbf{E}_0 = E_0\hat{\mathbf{x}}$ in the axial direction $\mathbf{x}$ and inhomogeneous density $n = n_0(x)$, $E_{0x} > 0$. Locally, Cartesian coordinates (x,y,z) are introduced with the z coordinate in the radial direction and y in the symmetrical azimuthal direction. The magnetic field is assumed to be predominantly in the radial direction, $\mathbf{B} = B_0(x)\hat{\mathbf{z}} + B_x(z)\hat{\mathbf{x}}$, though the $B_0 \gg B_x$.

The ions are assumed unmagnetized so that the magnetic field is omitted in the ion momentum equation,

$$m_i n_i \frac{d\mathbf{v}_i}{dt} = en_i\mathbf{E} - \nabla p_i. \tag{1}$$

The ion density is found from the continuity equation

$$\frac{\partial n_i}{\partial t} + \nabla \cdot (n_i \mathbf{v}_i) = 0. \tag{2}$$

Assuming $n_i = n_0 + \tilde{n}_i$ and $\mathbf{v}_i = \mathbf{v}_0 + \tilde{\mathbf{v}}_i$, with the zeroth order ion velocity defined as $v_0\hat{\mathbf{x}}$, Eqs. (1) and (2) can be linearized as

$$\frac{\partial \tilde{\mathbf{v}}_i}{\partial t} + v_0 \frac{\partial \tilde{\mathbf{v}}_i}{\partial x} = e\mathbf{E} - \frac{\nabla p_i}{m_i n_0}, \tag{3}$$

$$\frac{\partial \tilde{n}_i}{\partial t} + \mathbf{v}_0 \frac{\partial \tilde{n}_i}{\partial x} + n_0 \nabla \cdot \tilde{\mathbf{v}}_\mathbf{i} = 0. \tag{4}$$

We look for the solution in Fourier form $\sim e^{i(\mathbf{k}\cdot\mathbf{r}-\omega t)}$, which requires the Boussinesque quasi-classical approximation $k_x L_x \gg 1$, where $\mathbf{k} = (k_x, k_y, 0)$ is the wave-vector of perturbations. Considering only electrostatic perturbations and isothermal ions, Eqs. (3) and (4) give

$$\frac{\tilde{n}_i}{n_0} = \frac{e}{m_i} \frac{k_\perp^2 \phi}{(\omega - k_x v_0)^2 - k_\perp^2 v_{Ti}^2/2}, \tag{5}$$

where $v_{Ti}^2 = 2T_i/m_i$, and $k_\perp^2 = k_x^2 + k_y^2$.

The second term in the denominator of Eq. (5) is responsible for ion sound effect and Landau wave resonance. Note that we consider the perturbations aligned along the equilibrium magnetic field, so the conditions $\omega \gg (k_z v_{Te}, k_z v_{Ti})$ are satisfied both for ions and electrons.

The fluid theory is only justified in the non-resonant limit, $(\omega - k_x v_0)^2 \gg k_\perp^2 v_{Ti}^2$, so that Eq. (5) can be approximated as

$$\frac{\tilde{n}_i}{n_0} = \frac{e}{m_i} \frac{k_\perp^2 \phi}{(\omega - k_x v_0)^2}. \tag{6}$$

The general electron momentum equation is

$$m_e n_e \frac{d\mathbf{v}_e}{dt} = -en_e \left(\mathbf{E} + \frac{1}{c} \mathbf{v}_e \times \mathbf{B} \right) - \nabla p_e. \tag{7}$$

The electrons are magnetized and conditions

$$\omega \ll \omega_{ce}, \rho_e \ll L \tag{8}$$

are satisfied. The electron inertia term on the left hand side can be neglected for relatively low frequency long wavelength modes. This assumption eliminates low hybrid and modified tow-stream instabilities. Under these conditions, the electron velocity can be found in the form,

$$\mathbf{v}_e = \mathbf{v}_E + \mathbf{v}_{pe}, \tag{9}$$

where

$$\mathbf{v}_E = \frac{c}{B_0} \mathbf{b} \times \nabla \phi \tag{10}$$

is the $\mathbf{E} \times \mathbf{B}$ drift, and

$$\mathbf{v}_{pe} = -\frac{c}{enB_0} \mathbf{b} \times \nabla p_e \tag{11}$$

is the diamagnetic drift.

The fluid velocity from Eq. (9) is used in the continuity equation

$$\frac{\partial n_e}{\partial t} + \nabla \cdot (n_e \mathbf{v}_e) = 0, \tag{12}$$

giving the following equation for perturbed electron density

$$\frac{\partial}{\partial t} n + \mathbf{v}_E \cdot \nabla n - 2\mathbf{v}_E \cdot \nabla \ln B - 2n\mathbf{v}_{pe} \cdot \nabla \ln B = 0. \tag{13}$$

Here, the terms with gradients of magnetic field appear as a result of compressibility of the $= \mathbf{E} \times \mathbf{B}$ and diamagnetic velocity. The compressibility is calculated assuming low pressure plasmas so that terms due to the equilibrium plasma current are neglected, $\nabla \times \mathbf{B} = 0$, i.e., the equilibrium magnetic field is assumed to be the vacuum field. This results in

$$\nabla \cdot \mathbf{V}_E \simeq -2\mathbf{V}_E \cdot \nabla \ln B, \tag{14}$$

$$\nabla \cdot (n\mathbf{V}_{pe}) \simeq -2n\mathbf{V}_{pe} \cdot \nabla \ln B. \tag{15}$$

We would like to note that in a number of previous papers, e.g., Refs. 26 and 31, the compressibility is calculated by assuming the strictly one- dimensional magnetic field in the form $\mathbf{B} = B_0(x)\hat{\mathbf{z}}$ and the compressibility of electron flow was taken to be in the form $\nabla \cdot \mathbf{V}_E \simeq -\mathbf{V}_E \cdot \nabla \ln B$. One-dimensional magnetic field $\mathbf{B} = B_0(x)\hat{\mathbf{z}}$ has to be supported by a finite plasma current, which is not typical for Hall thruster conditions where the magnetic field with high accuracy is very close to the vacuum field.

In neglect of electron temperature fluctuations, the electron continuity equations results in the following form of the perturbed electron density:

$$\frac{n_e}{n_0} = \frac{\omega_* - \omega_D}{\omega - \omega_0 - \omega_D} \frac{e\phi}{T_e}. \tag{16}$$

Here, $\omega_D = k_y v_D$, $\omega_0 = k_y u_0$, and $\omega_* = k_y v_*$; v_D is the magnetic drift velocity, v_* is the electron diamagnetic drift velocity, and u_0 is the electric drift velocity in the equilibrium electric field, and

$$v_D = -2\frac{cT_e}{eB_0 L_B},$$

$$v_* = -\frac{cT_e}{eB_0 L_N},$$

$$\mathbf{u}_0 = -\hat{\mathbf{y}} \frac{cE_{0x}}{B_0},$$

where

$$\frac{1}{L_B} = \frac{\partial}{\partial x} \ln B(x),$$

$$\frac{1}{L_n} = \frac{\partial}{\partial x} \ln n_0(x).$$

Invoking quasineutrality and using Eqs. (6) and (16), we obtain the following dispersion relation[36]

$$\frac{\omega_* - \omega_D}{\omega - \omega_0 - \omega_D} = \frac{k_\perp^2 c_s^2}{(\omega - k_x v_{0i})^2}, \tag{17}$$

whose solutions are given by

$$\omega - k_x v_0 = \frac{1}{2} \frac{k_\perp^2 c_s^2}{\omega_* - \omega_D} \pm \frac{1}{2} \frac{k_\perp^2 c_s^2}{\omega_* - \omega_D} \times \sqrt{1 + 4\frac{k_x v_0}{k_\perp^2 c_s^2}(\omega_* - \omega_D) - 4\frac{k_y^2}{k_\perp^2}\rho_s^2 \Delta}. \tag{18}$$

The instability will occur for

$$\frac{k_y^2}{k_\perp^2} \rho_s^2 \Delta > \frac{1}{4},$$

where

$$\Delta = \frac{\partial}{\partial x} \ln \left(\frac{n_0}{B_0^2} \right) \left[\frac{eE_0}{T_e} + \frac{\partial}{\partial x} \ln (B_0^2) \right], \tag{19}$$

and $\rho_s^2 = T_e m_i c^2 / e^2 B_0^2$ is the so called ion-sound Larmor radius.

Equation (18) is similar to the electrostatic limit in Refs. 25 and 26. However, these authors did not include the compressibility of the electron diamagnetic drift due to finite electron temperature so the ω_D term in the denominator of the right hand side of Eq. (18) was absent. The electron diamagnetic drift was included in Ref. 31, however part of the

electron compressibility was omitted as described above. As a result, our dispersion equation (18) is similar in structure to Eq. (18) in Ref. 31, but numerical factors are different. The difference occurs because of the incomplete account of electron flow compressibility in Refs. 26 and 31.

Typically the electric field in the acceleration zone is large so that

$$\frac{eE_{0x}}{T_e} > \frac{\partial}{\partial x}\ln\left(B_0^2\right). \tag{20}$$

Then the condition for the instability is

$$\frac{\partial}{\partial x}\ln\left(\frac{n_0}{B_0^2}\right) > l_c^{-1}, \tag{21}$$

where the parameter l_c is defined as

$$l_c \equiv \frac{k_y^2}{k_\perp^2}\rho_s^2\left(\frac{eE_{0x}}{T_e} + \frac{\partial}{\partial x}\ln\left(B_0^2\right)\right), \tag{22}$$

and it is assumed that $E_{0x} > 0$.

For weak electric field

$$\frac{eE_{0x}}{T_e} < \frac{\partial}{\partial x}\ln\left(B_0^2\right), \tag{23}$$

the weaker instability may set in for

$$4\frac{k_y^2}{k_\perp^2}\rho_s^2\frac{\partial}{\partial x}\ln\left(\frac{n_0}{B_0^2}\right)\frac{\partial}{\partial x}\ln\left(B_0^2\right) > 1. \tag{24}$$

Equations (21) and (24) define the instability boundary in the (L_N, L_B) space. For purely azimuthal propagation ($k_x = 0$), and L_N and L_B of the same sign, the instability occurs when $L_B > 2L_N$. When L_N and L_B are of opposite signs, the instability will occur for negative L_B. There is no instability when L_B is positive but L_N is negative. Figure 1 shows the contour plot of the growth rate as a function of L_N and L_B for typical Hall thruster parameters ($B_0 = 150\,\mathrm{G}$, $n_0 = 10^{12}\,\mathrm{cm}^{-3}$, $u_0 = -4.75\times10^7\,\mathrm{cm/s}$, $T_e = 10\,\mathrm{eV}$, channel length $= 2.5\,\mathrm{cm}$) and typical characteristic lengths of the order of the channel length. The instability growth rate is in the megahertz range, increasing towards the marginal instability boundary $L_B = 2L_N$, close to which, the maximum growth rate is of the order of 50 MHz. The growth rates are smaller in the region where L_B is negative and L_N is positive. The growth rate for fixed values of L_B, as a function of L_N, is shown in Figs. 2 and 3 as a function of L_B. The growth rate sharply peaks as plasma parameters approach the instability boundary. Away from this boundary the growth rate decreases to values of the order of 0.5–1 MHz.

A characteristic feature of the dispersion relation (18) is a weak dependence of the real part of the frequency on the value of the equilibrium electric field, which enters only via the $k_x v_0$ term. For the generic case $L_N \simeq L_B \simeq L_T \simeq L_\phi$, the real and imaginary parts of the frequency scale as

$$\omega_r \simeq \omega_{ci} k_y L \tag{25}$$

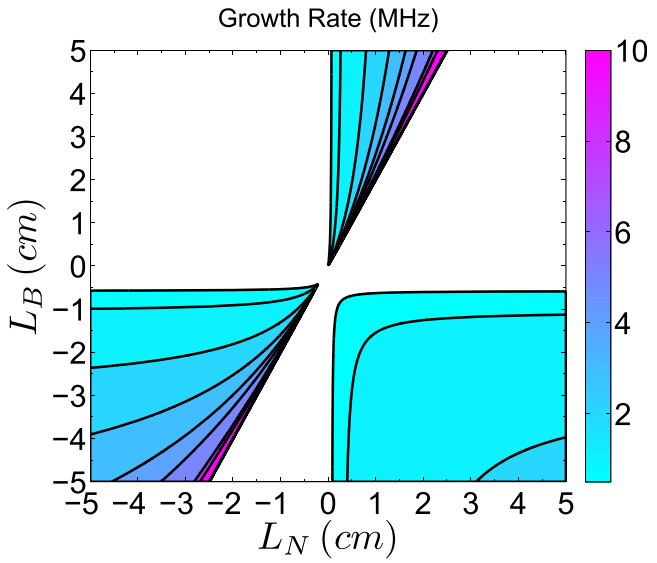

FIG. 1. Contour plot of the growth rate as a function of L_N and L_B.

and

$$\gamma \simeq k_\perp c_s\sqrt{\frac{eE_{x0}}{\left(L_B^{-1} - L_N^{-1}\right)}} \simeq k_\perp c_s\sqrt{\frac{e\phi_0}{T_e}}\ . \tag{26}$$

A notable feature of this instability is that the growth rates are maximal near the marginal stability boundary. The real part of the frequency also increases near the stability boundary and does not scale with the equilibrium $= \mathbf{E}\times\mathbf{B}$ electron drift velocity. It is important to note that the density gradient parameter L_N is intrinsically related to the electric field and, effectively, the electric field enters the dispersion relation (17) also via L_N.

The gradient-drift instability described by Eq. (17) persists also in the case when there is no gradient of the magnetic field. In this case, and assuming $k_x = 0$, the dispersion relation reduces to

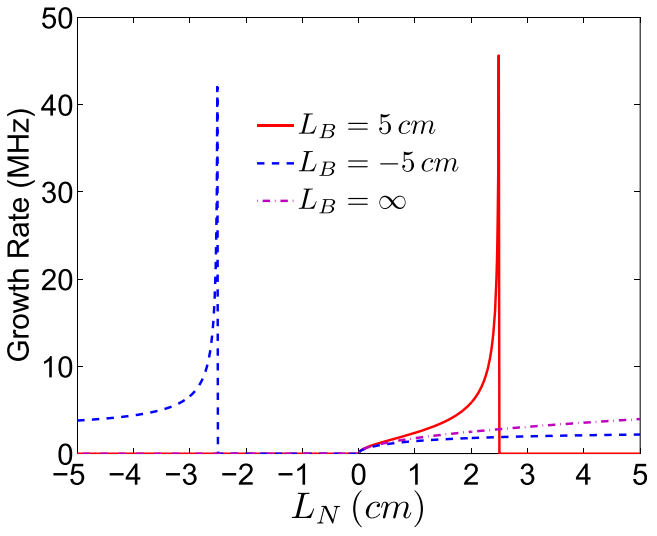

FIG. 2. Growth rate as a function of L_N for different values of L_B.

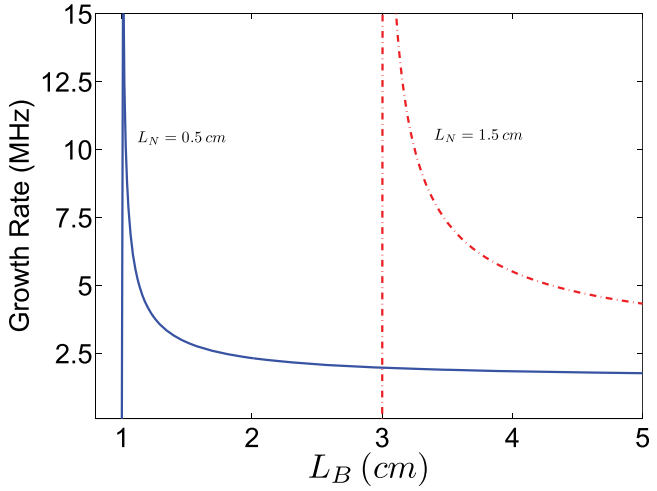

FIG. 3. Growth rate as a function of L_B for different values of L_N as given by the two fluid models. The vertical lines correspond to the instability boundary. As can be seen from the plots, the growth rate tends asymptotically to the values 1.56 MHz and 2.66 MHz, which correspond to the straight horizontal lines in Fig. 7.

$$\frac{\omega_*}{\omega-\omega_0}=\frac{k_\perp^2 c_s^2}{\omega^2}. \tag{27}$$

The solution of the dispersion relation (27) is

$$\omega=\frac{k_\perp^2 c_s^2}{2\omega_*}\left(1\pm\sqrt{1-\frac{4\omega_*\omega_0}{k_\perp^2 c_s^2}}\right). \tag{28}$$

The growth rate for the case of no magnetic field gradients is shown in Fig. 4. From Eq. (28), the conditions for instability are obtained as $(\partial/\partial x)\ln(n_0)E_0>0$ and

$$\frac{4|u_0|}{\omega_{ci}}\frac{1}{L_N}>1. \tag{29}$$

Instabilities driven by plasma density gradient and $\mathbf{E}_0\times\mathbf{B}_0$ drifts were studied in ionospheric physics,[37–39] though under different conditions, either with magnetized ions[38] or unmagnetized but strongly collisional ions.[39]

III. ELECTRON TEMPERATURE FLUCTUATIONS EFFECTS

The instability described in Refs. 26 and 31 and revisited in this paper is caused by an unfavorable combination of plasma density and magnetic field gradients. It is well known, however, that such instabilities can be affected by temperature gradients which were neglected by the authors of Refs. 26 and 31. Temperature gradient instabilities[40] are the main source of anomalous plasma transport in fusion plasmas[41] and may occur both in configurations with inhomogeneous magnetic field as well as in configurations with a uniform field.[42,43] In this section, we consider how the gradient drift instability in inhomogeneous magnetic field may be affected by temperature gradients, which are known to be significant for typical Hall thruster parameters.[44]

When fluctuations of the electron temperature are included, the electron continuity and momentum equations are complemented by the electron energy balance equation in the form

$$\frac{3}{2}\frac{dp}{dt}+\frac{5}{2}p\nabla\cdot\mathbf{v}+\nabla\cdot\mathbf{q}=0, \tag{30}$$

which includes the electron diamagnetic heat flux

$$\mathbf{q}=-\frac{5}{2}\frac{cp}{eB_0}\mathbf{b}\times\nabla T. \tag{31}$$

The electron energy equation, together with the electron continuity equation, quasineutrality and the equations for ion component constitutes a three-field (n,T,ϕ) fluid model for gradient-drift instability, while in the two-field model, only the electron density and electrostatic potential were included (n,ϕ). Taking into account finite electron temperature fluctuations, the electron density equation (13) results in

$$-(\omega-\omega_0-\omega_D)\frac{\tilde{n}_e}{n_0}+\omega_D\frac{\tilde{T}_e}{T_0}=-(\omega_*-\omega_D)\frac{e\phi}{T_e}. \tag{32}$$

The temperature evolution can be found from the energy balance equation (30) or equivalently from the temperature equation,

$$\frac{3}{2}n\frac{dT}{dt}+p\nabla\cdot\mathbf{v}+\nabla\cdot\mathbf{q}=0. \tag{33}$$

Using Eqs. (9) and (31), Eq. (33) is reduced to the form

$$\frac{3}{2}n\left(\frac{\partial T}{\partial t}+\mathbf{v}_E\cdot\nabla T\right)-2p\mathbf{v}_E\cdot\nabla\ln B+\frac{2cT}{eB_0}\nabla\ln B\cdot\mathbf{b}\times\nabla p+\frac{5cp}{eB_0}\nabla\ln B\cdot\mathbf{b}\times\nabla T=0. \tag{34}$$

In linearized form, one gets the equation,

$$\omega_D\frac{\tilde{n}_e}{n_0}+\left(\frac{7}{2}\omega_D-\frac{3}{2}(\omega-\omega_0)\right)\frac{\tilde{T}_e}{T_e}=\left(\omega_D-\frac{3}{2}\omega_{*T}\right)\frac{e\phi}{T_e}, \tag{35}$$

where

$$\omega_{*T}=-\frac{k_y cT_{e0}}{eB_0L_T} \tag{36}$$

and

$$\frac{1}{L_T}=\frac{\partial\ln T_{e0}}{\partial x}.$$

The coupled equations (32) and (35) for density and temperature can be solved giving the following equations for the electron temperature and density:

$$\frac{\tilde{T}_e}{T_e}=\frac{(\omega-\omega_0-\omega_D)\omega_{*T}-\frac{2}{3}(\omega-\omega_0-\omega_*)\omega_D}{(\omega-\omega_0)^2-\frac{10}{3}\omega_D(\omega-\omega_0)+\frac{5}{3}\omega_D^2}\frac{e\phi}{T_e}, \tag{37}$$

$$\frac{n_e}{n_0}=\frac{-(\omega-\omega_0)(\omega_D-\omega_*)+\omega_D\left(\omega_{*T}-\frac{7}{3}\omega_*\right)+\frac{5}{3}\omega_D^2}{(\omega-\omega_0)^2-\frac{10}{3}\omega_D(\omega-\omega_0)+\frac{5}{3}\omega_D^2}\frac{e\phi}{T_e}. \tag{38}$$

One should note that the models of the electron density and electron temperature used in our paper, as well as in previous papers, completely neglect the parallel electron dynamics in the direction of the equilibrium magnetic field. Using Eqs. (6) and (38), along with the quasineutrality condition, the following cubic dispersion relation is obtained:

$$\frac{-(\omega-\omega_0)(\omega_D-\omega_*)+\omega_D\left(\omega_{*T}-\frac{7}{3}\omega_*\right)+\frac{5}{3}\omega_D^2}{(\omega-\omega_0)^2-\frac{10}{3}\omega_D(\omega-\omega_0)+\frac{5}{3}\omega_D^2} = \frac{k_\perp^2 c_s^2}{(\omega-k_x v_{0i})^2}. \tag{39}$$

It is important to note that temperature fluctuations remain finite even in plasma without temperature gradients. Finite temperature fluctuations occur as a result of plasma compression in inhomogeneous magnetic field. Note that plasma dynamics is not adiabatic due to finite compressibility of the heat flux, $\nabla \cdot \mathbf{q} \neq 0$: in magnetized plasmas with nonuniform magnetic field the flow of plasma density and energy are different. As a result even in the limit of $L_T = \infty$, the three-field model predicts different stability picture as compared to the two-field model. In a homogeneous magnetic field, when $\omega_D = 0$, the dispersion relation form Eq. (39) reduces to Eq. (27) and temperature gradient effects are not important.

Equation (39) is solved numerically to study the effect of the gradients of the electron temperature in the three-field model. The qualitative landscape of the instability in (L_N, L_B) plane is similar to the results from the two-field model in Fig. 1, though, quantitatively, the growth rate values and the behavior change (Fig. 5).

The growth rate profile as function of L_B and L_T is shown on the contour plot in Fig. 6 for $L_N = 0.5$ cm and $L_N = 1.5$ cm. For these characteristic lengths of density gradient, the maximum growth rate for positive values of L_T is of the order of 15 MHz and 22 MHz, respectively, attained close to the instability boundary. Also, it is clear from this figure that the stability window widens for increasing positive values of L_N. For the positive values of L_N used, the

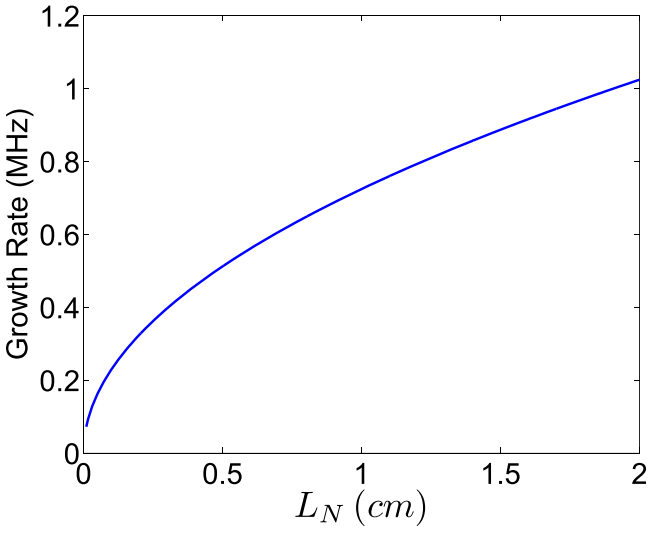

FIG. 4. Growth rate as a function of L_N for the case with no gradients of the magnetic field.

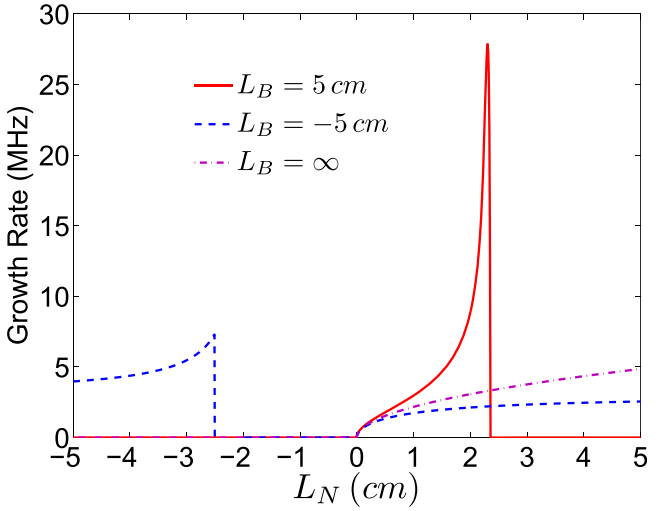

FIG. 5. Growth rate as a function of L_N for different values of L_B when L_T is 1 cm.

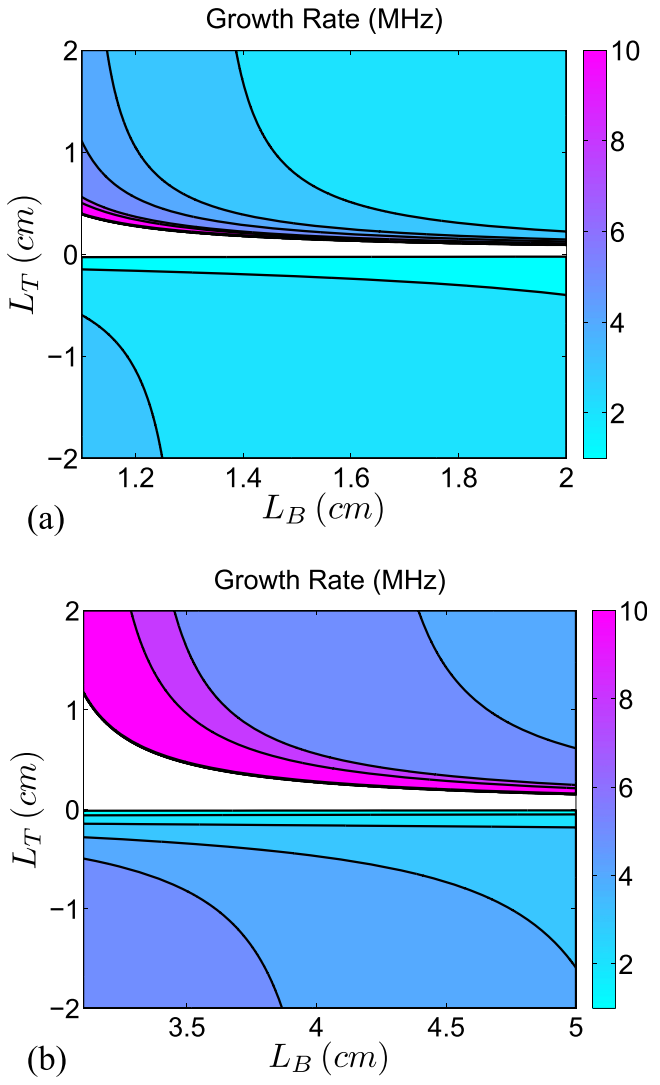

FIG. 6. Contour plot of the growth rate as a function of L_B and L_T for $L_N = 0.5$ cm and $L_N = 1.5$ cm.

instability is also possible for negative gradients of temperature. The value of the growth rate in this case is in general smaller that for positive values of L_B.

The Fig. 7 shows the effects of temperature in three-field model. For lower values of L_B (strong magnetic field gradient), the instability occurs only for a narrow window of L_T values. When the characteristic length L_B increases, the instability regions becomes wider and the growth rate to decrease from a maximum value of around 10 MHz to the value of 1.56 MHz for $L_N = 0.5$ cm and from around 20 MHz to 2.66 MHz for $L_N = 1.5$ cm. The latter values correspond to the limit of no magnetic field gradient ($L_B \to \infty$). The same limit is recovered from the two-field model as shown in Fig. 3. One of the important results of the three-field model is the prediction of the stabilization of the instability for larger of the temperature gradient. On the other hand, in unstable regions, the three-field model predicts higher growth rates compared to the two-field model. Comparison between the two-field and three-field models can be seen from Fig. 7 which shows the growth rate as a function of the temperature gradient L_T for different values of L_B and L_N. This behaviour is to be compared with the results of the two-field shown in Fig. 3, where the growth rate fluid model is shown as a function of L_B, for two values of L_N used in Fig. 7.

Another important difference between the two field model and the three field model is the growth rates predicted for small values of the electric field, as the ones near the anode region in a Hall thruster. The dependence of the growth rate on the electric field is drawn in Fig. 8. In both cases, the growth rate increases with increasing electric field and decreases with increasing value of L_B, which corresponds to regions away from the instability boundary. In the regions with electric field close to zero, the two field model predicts a non zero growth rate, while the three field model predicts a small stable region close to $E_0 = 0$. This stable region becomes narrower as L_B increases. Close to this stability boundary, the growth rate increases sharply, reaching a peak and then falls and continues to grow with the electric field. Also, when the parameter L_T increases, while L_B and L_N remain fixed, the growth rate decreases, but the stable region becomes wider, showing that the effect of the temperature gradients from one side to reduce the instability when L_T

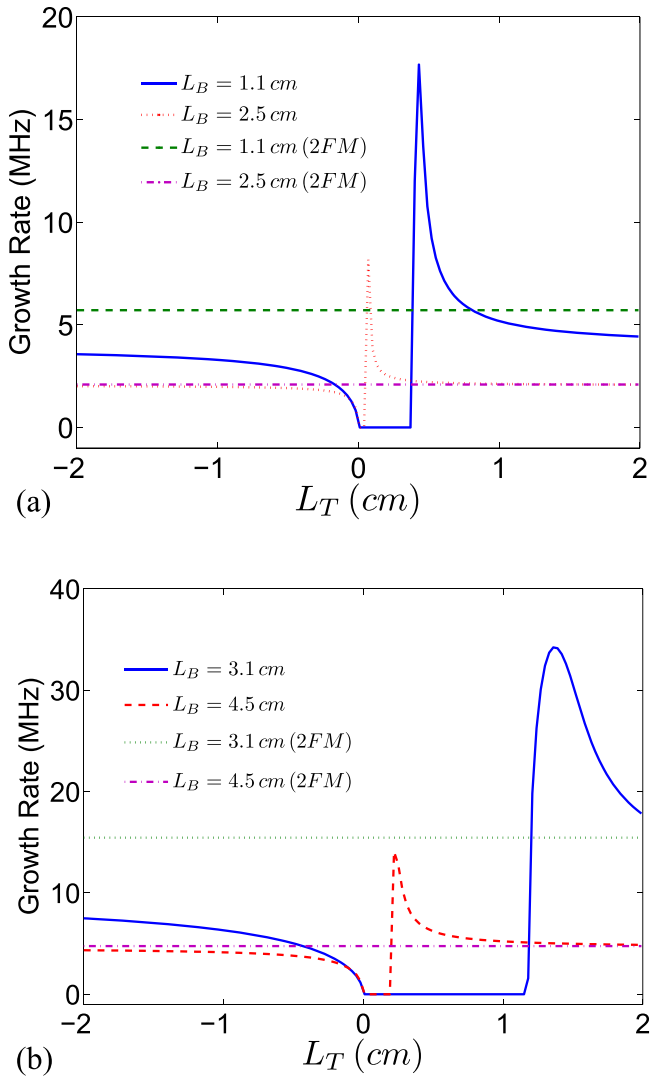

FIG. 7. Growth rate as a function of L_T for (a) $L_N = 0.5$ cm and (b) $L_N = 1.5$ cm, for different values of L_B. The straight lines correspond to the values predicted by the two-field model.

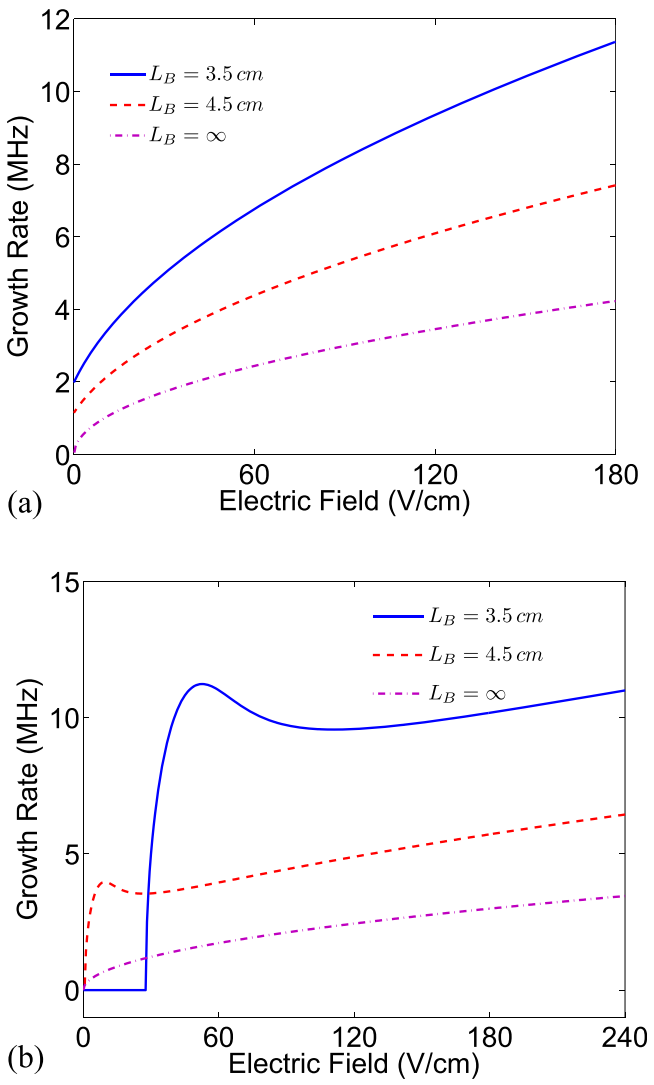

FIG. 8. Growth rate as a function of the electric field for $L_N = 1.5$ cm as predicted by (a) the two-field model and (b) the three-field model, $L_T = 1$ cm.

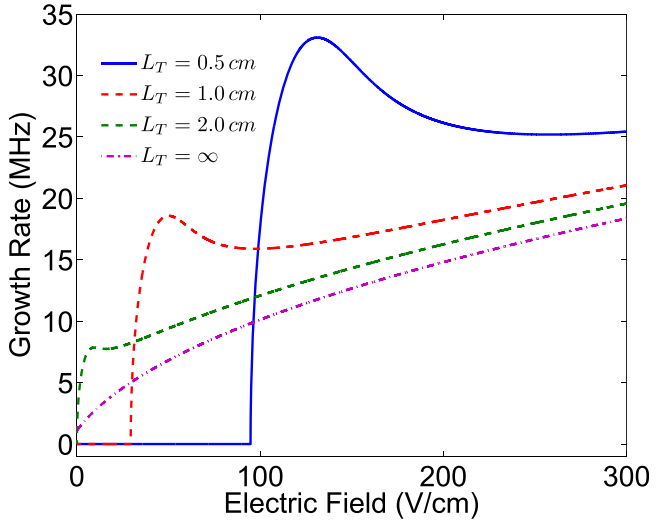

FIG. 9. Growth rate as a function of electric field for $L_N = 2.0$ cm, $L_B = 4.5$ cm and different values of L_T.

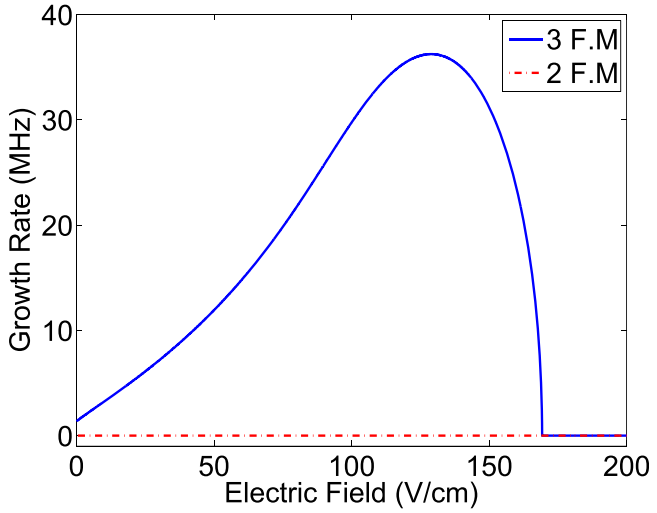

FIG. 10. Growth rate as a function of electric field as predicted by the three-field model: $L_N = 1.5$ cm, $L_B = 2.9$ cm, $L_T \to \infty$. Two-field model predicts no instability for these parameters.

grows, but at the same time, to create regions of stability in regions where L_T is small, as can be seen in Fig. 9.

This situation can be clearly appreciated in Fig. 10, where the growth rate as a function of the electric field is plotted for the parameters $L_N = 1.5$ cm and $L_B = 2.9$ cm. For these parameters, the two field model predicts stability, while the three-field model predicts instability for certain values of the electric field.

IV. SUMMARY

Understanding of the turbulent electron mobility requires a detailed knowledge of the spectra of unstable modes and their saturation levels. Quantitative information about the conditions for linear instabilities and mode eigenvalues (real part of the frequencies and growth rates) is, thus, of interest. Earlier works in instabilities in Hall thruster plasmas revealed the plasma density and magnetic field gradients as important sources of long wavelength plasma instabilities. We have revisited this problem and derived a modified criterion for this instability as discussed in Sec. II. We have extended the fluid model to include the dynamics of electron temperature and have developed a three-field fluid model that includes the electron energy equation. The inclusion of two moments, density and temperature, provides a more accurate model of the electron response. Such two moments (n, T) model amounts to the two-pole approximation of the exact kinetic response and provide a reasonably accurate description of the exact kinetic response away from the resonances.[45] Such models were shown to be successful in describing a wide class temperature gradient modes in fusion plasmas.[45] The possible role of resonances has to be investigated with a kinetic model that will be reported somewhere else.

Our analysis shows the effects of temperature fluctuations included in two-moment (n,T), or equivalently, in three-field model, $(n, T,)\phi$, may significantly modify the instabilities of Hall plasmas with unmagnetized ions, in particular, near the marginal stability boundary. It also predicts the instability for the parameters where two-field model is stable. It is important to note that gradient-drift instabilities as predicted by our model are mostly aperiodic modes with $\gamma \gg \omega_r$. The real part of the frequency does not explicitly depend on the equilibrium electric field (only via explicit dependence via L_N and L_B). Two-field model predict the scaling for the real part of the mode frequency $\omega_r \simeq -(k_\perp^2/k_y)\omega_{ci}(L_N^{-1} - 2L_B^{-1})^{-1}$, see Eq. (18). The main features of this scaling are similar in the three-field model, though it could be modified near the marginal stability boundary. Experimental observations[5,9,29] show inverse dependence on the magnetic field and show increase with the electric field. The scaling above does not show these features, though they might appear via implicit dependence on L_N. In unstable case $(L_N^{-1} - 2L_B^{-1}) > 0$, and real part of the mode $\omega_r < 0$, which is consistent with the direction of the equilibrium $\mathbf{E} \times \mathbf{B}$ drift, though the frequency is significantly lower than $k_y u_0$. Similar trend was observed experimentally,[35] where it was explained on a basis of the cyclotron instabilities driven by the equilibrium electron drift.

Similar to the previous work,[25,26,31] we have neglected the electron inertia in the transverse electron current as well the parallel electron flow. The latter assumption is equivalent to the condition that the wave vector component $k_{||}$ along the magnetic field is zero, while the neglect of electron inertia eliminates low hybrid modes. These conditions are equivalent to the model of thermalized magnetic field lines introduced in Refs. 1–3. In Part II, we will apply the obtained stability criteria to the realistic configurations of plasma parameters in some Hall thruster experiments.

[1]A. I. Morozov, Plasma Phys. Rep. **29**, 235 (2003).
[2]A. Morozov and V. Savelyev, in *Reviews of Plasma Physics*, edited by B. Kadomtsev and V. Shafranov (Kluver, New York, 2000), Vol. 21, pp. 203–391.
[3]D. Goebel and I. Katz, *Fundamentals of Electric Propulsion: Ion and Hall Thrusters*, JPL Space Science and Technology Series (Wiley, 2008).
[4]M. Keidar and I. Beilis, IEEE Trans. Plasma Sci. **34**, 804 (2006).
[5]A. Lazurenko, G. Coduti, S. Mazouffre, and G. Bonhomme, Phys. Plasmas **15**, 034502 (2008).

[6]R. Spektor, in *Proceedings of 30th International Electric Propulsion Conference, Florence* (Electric Rocket Propulsion Society, Cleveland, OH, 2007), IEPC Paper No. 2007–70.
[7]G. N. Tilinin, Sov. Phys. Tech. Phys. **22**, 974 (1977).
[8]E. Y. Choueiri, Phys. Plasmas **8**, 1411 (2001).
[9]A. Lazurenko, L. Albarede, and A. Bouchoule, Phys. Plasmas **13**, 083503 (2006).
[10]S. Tsikata, N. Lemoine, V. Pisarev, and D. M. Gresillon, Phys. Plasmas **16**, 033506 (2009).
[11]A. B. Mikhailovskii, *Electromagnetic Instabilities in an Inhomogeneous Plasma* (Taylor & Francis, 1992).
[12]R. C. Davidson, N. T. Gladd *et al*., in *Plasma Physics and Controlled Nuclear Fusion Research 1976, Sixth Conference Proceedings*, edited by IAEA (IAEA, Vienna, 1977), Vol. 3, pp. 113–121.
[13]B. R. Appleton, C. D. Moak, T. S. Noggle, and J. H. Barrett, Phys. Rev. Lett. **28**, 1307 (1972).
[14]N. A. Krall and P. C. Liewer, Phys. Rev. A **4**, 2094 (1971).
[15]D. G. Lominadze and K. N. Stepanov, Sov. Phys. Tech. Phys. **9**, 1408 (1965).
[16]A. B. Mikhailovskii and V. S. Tsypin, JETP Lett. **3**, 247 (1966).
[17]J. D. Huba and C. S. Wu, Phys. Fluids **19**, 988 (1976).
[18]N. A. Krall and J. B. McBride, Phys. Fluids **19**, 1970 (1976).
[19]R. C. Davidson and N. T. Gladd, Phys. Fluids **18**, 1327 (1975).
[20]A. Fruchtman, Phys. Fluids B **1**, 422 (1989).
[21]M. Lampe, W. M. Manheimer, J. B. McBride, J. H. Orens, K. Papadopoulos, R. Shanny, and R. N. Sudan, Phys. Fluids **15**, 662 (1972).
[22]M. Lampe, W. M. Manheimer, J. B. McBride, J. H. Orens, R. Shanny, and R. N. Sudan, Phys. Rev. Lett. **26**, 1221 (1971).
[23]A. Ducrocq, J. C. Adam, A. Heron, and G. Laval, Phys. Plasmas **13**, 102111 (2006).
[24]T. D. Kaladze, D. G. Lominadze, and K. N. Stepanov, Sov. Phys. JETP **7**, 196 (1972).
[25]A. I. Morozov, Y. V. Esipchuk, A. Kapulkin, V. Nevrovskii, and V. A. Smirnov, Sov. Phys. Tech. Phys. **17**, 482 (1972).
[26]Y. V. Esipchuk and G. N. Tilinin, Sov. Phys. Tech. Phys. **21**, 417 (1976).
[27]E. Chesta, N. B. Meezan, and M. A. Cappelli, J. Appl. Phys. **89**, 3099 (2001).
[28]D. Escobar and E. Ahedo, in *Proceedings of 32nd International Electric Propulsion Conference, Wiesbaden* (Electric Rocket Propulsion Society, Cleveland, OH, 2011), IEPC Paper No. 2011-196.
[29]A. A. Litvak, Y. Raitses, and N. J. Fisch, Phys. Plasmas **11**, 1701 (2004).
[30]A. A. Litvak and N. J. Fisch, Phys. Plasmas **8**, 648 (2001).
[31]A. Kapulkin and M. M. Guelman, IEEE Trans. Plasma Sci. **36**, 2082 (2008).
[32]J. Kurzyna, S. Mazouffre, A. Lazurenko, L. Albarede, G. Bonhomme, K. Makowski, M. Dudeck, and Z. Peradzynski, Phys. Plasmas **12**, 123506 (2005).
[33]M. Prioul, Ph.D. dissertation, University of Orleans, 2002.
[34]J. C. Adam, A. Heron, and G. Laval, Phys. Plasmas **11**, 295 (2004).
[35]S. Tsikata, C. Honore, N. Lemoine, and D. M. Gresillon, Phys. Plasmas **17**, 112110 (2010).
[36]A. Smolyakov, W. Frias, E. Raitses, and I. Kaganovich, in *Proceedings of 32nd International Electric Propulsion Conference, Wiesbaden* (Electric Rocket Propulsion Society, Cleveland, OH, 2011), IEPC Paper No. 2011–271.
[37]A. Simon, Phys. Fluids **6**, 382 (1963).
[38]J. D. Huba, S. L. Ossakow, P. Satyanarayana, and P. N. Guzdar, J. Geophys. Res. [Space Phys.] **88**, 425, doi:10.1029/JA088iA01p00425 (1983).
[39]R. N. Sudan, A. V. Gruzinov, W. Horton, and N. Kukharkin, Phys. Rep. **283**, 95 (1997).
[40]B. Coppi, M. N. Rosenbluth, and R. Z. Sagdeev, Phys. Fluids **10**, 582 (1967).
[41]J. W. Connor, Nucl. Fusion **26**, 193 (1986).
[42]W. Horton, D. I. Choi, and W. M. Tang, Phys. Fluids **24**, 1077 (1981).
[43]A. Jarmen, P. Andersson, and J. Weiland, Nucl. Fusion **27**, 941 (1987).
[44]D. Staack, Y. Raitses, and N. J. Fisch, Appl. Phys. Lett. **84**, 3028 (2004).
[45]J. Weiland, *Collective Modes in Inhomogeneous Plasmas: Kinetic and Advanced Fluid Theory* (Taylor & Francis, 1999).